Title
Lentiviral gene therapy for X-linked chronic granulomatous disease.

Permalink
https://escholarship.org/uc/item/7b61w03m

Journal
Nature medicine, 26(2)

ISSN
1078-8956

Authors
Kohn, Donald B
Booth, Claire
Kang, Elizabeth M
et al.

Publication Date
2020-02-01

DOI
10.1038/s41591-019-0735-5

Peer reviewed

Lentiviral gene therapy for X-linked chronic granulomatous disease

Donald B. Kohn[1,*], **Claire Booth**[2], **Elizabeth M. Kang**[3], **Sung-Yun Pai**[4], **Kit L. Shaw**[1], **Giorgia Santilli**[2], **Myriam Armant**[4], **Karen F. Buckland**[2,a], **Uimook Choi**[3], **Suk See De Ravin**[3], **Morna J. Dorsey**[5], **Caroline Y. Kuo**[1], **Diego Leon-Rico**[2], **Christine Rivat**[2], **Natalia Izotova**[2], **Kimberly**

[*]**Corresponding authors: Donald B Kohn,** University of California, Los Angeles, Depts. of Microbiology, Immunology & Molecular Genetics (M.I.M.G.) and Pediatrics, 615 Charles E. Young Drive East, 290D BSRB, Los Angeles, CA, USA 90027, USA. dkohn@mednet.ucla.edu. Tel: + 00 1 310-794-1964; **Adrian J Thrasher,** University College London Great Ormond Street Institute of Child Health and Great Ormond Street Hospital NHS Foundation Trust, Department of Molecular & Cellular Immunology, 30 Guilford Street, London, WC1N 1EH, UK. a.thrasher@ucl.ac.uk. Tel: +44 (0)20 7905 2660 (Ex. 42660).
[a]On behalf of the Net4CGD consortium
[b]Current address: City of Hope, Beckman Research Institute, Duarte, CA, USA

Gilmour[2], **Katie Snell**[2], **Jinhua Xu-Bayford Dip**[2], **Jinan Darwish**[2], **Emma C. Morris**[6], **Dayna RN Terrazas**[1], **Leo D. Wang**[4,b], **Christopher A. Bauser**[7,a], **Tobias Paprotka**[7], **Douglas B. Kuhns**[8], **John Gregg**[9], **Hayley E. Raymond**[9], **John K. Everett**[9], **Geraldine Honnet**[10,a], **Luca Biasco**[2], **Peter E. Newburger**[11], **Frederic D. Bushman**[9], **Manuel Grez**[12,a], **H. Bobby Gaspar**[2,13,a], **David A. Williams**[4], **Harry L. Malech**[3], **Anne Galy**[10,a,14], **Adrian J. Thrasher**[2,a,*]

[1]University of California, Los Angeles, CA, USA

[2]Great Ormond Street Institute of Child Health and Great Ormond Street Hospital NHS Foundation Trust, London, UK

[3]Laboratory of Clinical Immunology and Microbiology, National Institute of Allergy and Infectious Diseases, National Institutes of Health, Bethesda, MD, USA

[4]Boston Children's Hospital, Harvard Medical School, Boston, MA, USA

[5]University of California, San Francisco, CA, USA

[6]University College London Hospitals NHS Foundation Trust, London, UK

[7]Eurofins Genomics Sequencing Europe, Konstanz, Germany

[8]Leidos Biomedical Research, Inc. Frederick National Laboratory for Cancer Research, Frederick, MD, USA

[9]University of Pennsylvania, Philadelphia, PA, USA

[10]Genethon, Evry, France

[11]University of Massachusetts Medical School, Worcester, MA, USA

[12]Georg-Speyer Haus, Frankfurt, Germany

[13]Orchard Therapeutics, London, UK

[14]Inserm, University of Evry, Université Paris Saclay (UMR_S951), Genethon, Evry, France

Introductory Paragraph

Chronic granulomatous disease (CGD) is a rare inherited disorder of phagocytic cells[1,2]. We report initial results of nine severely affected X-linked CGD (X-CGD) patients who received *ex vivo* autologous CD34+ hematopoietic stem and progenitor cell-based lentiviral gene therapy following myeloablative conditioning in first-in-man studies (Trial registry numbers: NCT02234934, NCT01855685). Primary objectives were to assess safety and evaluate efficacy and stability of biochemical and functional reconstitution in the progeny of engrafted cells at 12 months. The secondary objectives included the evaluation of augmented immunity against bacterial and fungal infection, and assessment of hematopoietic stem cell transduction and engraftment. Two enrolled patients died within 3 months of treatment from pre-existing comorbidities. At 12 months, six of the seven surviving patients demonstrated stable vector copy number (0.4–1.8 copies/neutrophil) and persistence of 16–46% oxidase-positive neutrophils. There was no molecular evidence of clonal dysregulation or of transgene silencing. Surviving patients have had no new CGD-related infections, and six have been able to discontinue CGD-related antibiotic prophylaxis. The primary objective was met in 6 of the 9 patients at 12 months follow-up suggesting that autologous gene therapy is a promising approach for CGD patients.

Introduction

X-CGD is caused by mutations in *CYBB* encoding the gp91phox subunit of the phagocyte nicotinamide adenine dinucleotide phosphate (NADPH)-oxidase (NOX2). Patients are susceptible to recurrent life-threatening infections, impacting their quality of life and life-expectancy. Allogeneic hematopoietic stem cell transplantation (HSCT) can be curative, and recent advances have improved the results from this treatment considerably[3,4]. Clinical trials of hematopoietic stem and progenitor cell (HSPC) gene therapy were first initiated with gammaretroviral (γ-RV) vectors.[5,6] However, clonal expansion of gene-corrected cells mediated by potent enhancer elements in the γ-RV long-terminal repeats (LTRs)[5,7], eventually lead to leukoproliferative complications. In addition, CpG dinucleotide promoter methylation lead to silencing of transgene expression[7]. To retain the efficacy of gene therapy for X-CGD, but minimize mutagenic risk, a self-inactivating lentiviral vector called G1XCGD was developed (Fig. 1a, full sequence shown in Extended Data 1). To enhance the safety of this vector, a novel chimeric internal promoter was used to preferentially drive gp91phox expression at high levels in phagocytes [8,9]. Complementary clinical studies were initiated, including a multicenter trial in the USA, a UK study and compassionate-use program with nearly identical clinical protocols, eligibility criteria, myeloablative conditioning, stem cell product manufacturing methods, vector batches, and post-transplant analyses.

Results

Recovery of functional oxidase activity in patients

Ongoing clinical studies of gene therapy with G1XCGD were initiated in the UK ($n = 3$, plus one compassionate-use patient) and in the USA ($n = 5$). Dates of therapy are provided in Table 1. Patients 1, 3, 5, and 9 were treated in the UK. Patients 2, 4, 6, 7, and 8 were treated in the USA. The patients were all male with severe deficiency of gp91phox and absent NADPH-oxidase activity. They ranged in age from 2 to 27 years, and six of the nine were >18 years of age at entry. All patients had clinical histories of severe X-CGD-related infections, some active at the time of treatment, and several had chronic inflammatory complications (Table 1). Patients were followed until death or for a minimum of 12 months, with a maximum follow-up of 36 months. Drug products were manufactured from granulocyte colony-stimulating factor (G-CSF) and Plerixafor-mobilized leukaphereses, and infused after myeloablative conditioning (Table S1, see online methods). Drug product infused for the nine patients achieved final CD34$^+$ cell doses of 6.5–32.6×10^6/kg (Table S2, Extended Data 2).

Within 1 month of gene therapy, corrected circulating neutrophils were detectable in peripheral blood (Fig. 2a, 2b; assays conducted in a subset of patients, once at each time point for each patient). Dihydrorhodamine (DHR) fluorescent assays were applied serially to follow the levels of corrected neutrophils. DHR+ activity was observed in >15% of polymorphonuclear neutrophils in all patients within 1 month Fig. 2c and Extended Data 3a. Follow-up demonstrated sustained, stable persistence of oxidase-positive neutrophils in six of seven surviving patients; the percentage of oxidase-positive neutrophils at 12 months was

16–46% in these individuals, indicating that the primary objective of evaluating the efficacy in the progeny of engrafted cells and stability at 12 months had been met. Expression of transgene-derived gp91phox was confirmed by flow cytometry as occurring in a percentage of circulating neutrophils that paralleled the DHR data (data not shown). Quantification of NADPH-oxidase generation of superoxide was performed by measurement of neutrophil-stimulated reduction of ferricytochrome c and corrected for the percentage of functional cells. These results demonstrated that the level of activity was within, or just below, the expected normal range of superoxide production per activated neutrophil (Fig. 2d; assays conducted in a subset of patients, once at each time point for each patient), further strengthening the conclusion that the primary objective relating to efficacy was met.

Vector integration

Following reinfusion, VCN remained stable in neutrophils in six patients over the course of follow-up, suggestive of successful transduction and engraftment of HSPCs (Fig. 2e, Extended Data 3b). In general, the percentage of DHR-positive neutrophils increased linearly with granulocyte VCN (Fig. 2f). VCN also remained stable in other cell lineages (Extended Data 4). One patient (Patient 5, who required three attempts to collect CD34+ cells) had a high initial VCN and a high percentage of DHR-positive neutrophils, but a decrease in VCN and a parallel decrease in the percentage of oxidase-positive neutrophils (<0.5%) over 18 months of follow-up. The patient remained clinically well at last follow-up on prophylactic antimicrobials.

Longitudinal analysis of vector integration-site distributions was carried out for the nine patients over 3 months–3 years of sampling. More than 106 million sequence reads identified 724,685 unique integration sites in multiple cell types (Fig. 3a). Lentiviral vector integration was favored in transcription units and transcription-associated features, as seen previously[10]. The analysis documented highly polyclonal populations of gene-modified cells; after 1 year, an average of 9,482 unique integration sites were detected in peripheral blood mononuclear cells (PBMCs; assayed in Patients 2, 4, 6 and 7). Mathematical reconstructions of population sizes using Chao1 estimation[11] with PMBC samples from these same four patients 12 months after treatment suggest an average of at least 69,034 progenitor cells were delivering gene-corrected cells to peripheral blood at 1 year (Extended Data 5). In a previous gene therapy trial to treat CGD, which used a γ-RV vector, clones with integration sites in MECOM (MDS/EVI1) expanded by 1 year in peripheral blood to comprise more than 20% of cells in the first patient and more than 80% of cells in the second[7], and were implicated in later adverse events. In this study, with the lentiviral G1XCGD vector and assayed in neutrophils, the most abundant clones did not harbor integration sites in or near these genes (Fig 3b), and no clone at genes of concern in the previous trial expanded to comprise more than 0.3% of the total population in any cell type (Extended Data 6). In addition, there was no evidence of significant gene silencing, nor of CpG dinucleotide methylation in vector regulatory sequences (Fig. 3c)

Clinical outcomes

The infusion of the medicinal drug product containing genetically modified cells was well tolerated and there were no infusion-related adverse events. All patients experienced typical

conditioning-related events, including transient neutropenia, thrombocytopenia and/or mucositis. There were two deaths: one (Patient 1) due to hyperacute sterile pneumonitis 9 weeks after infusion of gene-corrected cells on a background of prior extensive *Aspergillus* lung disease and pneumonectomy; and the other (Patient 8) due to a fatal intracranial bleed post-transplant associated with refractory autoimmune platelet destruction precipitated by previous alloimmunization to multiple granulocyte transfusions. Pre-mortem magnetic resonance imaging showed the bleed to be centered at a site of metastatic fungal infection. These deaths were not considered related to the drug product. There was one serious adverse reaction, consistent with similar cases in other diseases treated with gene therapy and transplant[12,13]: Patient 5 experienced immune reconstitution inflammatory syndrome at initial engraftment of functional neutrophils, manifesting as a pericardial effusion and abdominal pain, which was fully resolved with steroid cover. In the remaining patients, there were two adverse events recorded after transplant: one patient (Patient 2) developed transient symptoms of gastric outflow obstruction 3–4 months after gene therapy that had been a recurrent pre-transplant problem; there was no evidence of outflow obstruction on endoscopy and symptoms did not recur. Another patient (Patient 6) had several spontaneous pneumothoraces, related to pre-transplant bronchiectasis, established pulmonary fibrosis and was markedly lymphopenic at enrollment, having received several courses of corticosteroid for inflammatory pulmonary disease. Of the patients who had colitis at some time prior to gene therapy, none have had clinical recurrences to date. In one patient (Patient 3) who had active colitis with a perianal fistula and perineal ulceration at the time of gene therapy, there was resolution of the lesion soon after gene therapy with no recurrence.

After 2,036 patient days (approximately 66 patient months), all seven surviving patients remained clinically well without new CGD-related infections. The six patients with stable DHR+ neutrophils >10% were no longer receiving CGD-related prophylactic antibiotic or antifungal treatment (some patients continued to receive penicillin V or equivalent prophylaxis per individual institution-specific protocols for patients who received myeloablative conditioning). Patient 6 remained on antibiotic prophylaxis due to pre-existing lung disease and lymphopenia but is currently off antifungal therapy (Table 1). The secondary objectives to assess immunologic reconstitution and patient health (US protocol) and immunity against bacterial and fungal infection (UK protocol) were therefore met.

Discussion

Following gene therapy, all patients with successful engraftment remain stable through to the last follow-up (up to 3 years in three patients). Seven patients remained free of new infectious complications, and six had sustained presence of neutrophils and restored NADPH-oxidase activity with no evidence of transcriptional silencing of the integrated vector genome or clonal expansion. Two patients died within 3 months of gene therapy likely due to pre-existing disease-related complications present at transplant and unrelated to the drug product itself. The other seven patients have remained well, apart from persistent chronic fibrotic pulmonary problems in one individual (Patient 6).

One patient (Patient 5), a pediatric patient, initially achieved high levels of neutrophil recovery although the levels of activity declined over several months, suggesting that only a

low frequency of long-term transduced HSCs had engrafted, possibly as a result of chronic inflammation[14]. This patient had also received long-term linezolid, an antimicrobial agent with known myelosuppressive activity[14], which may also have contributed to difficulty recovering sufficient CD34+ cells for transduction, requiring three separate attempts. Since this analysis was performed, four additional patients (aged 3, 8, 11, and 31 years) have been treated in the USA with cryopreserved cells, with no product-related complications. At the last follow-up (2–9 months post-treatment), all were well, with no new CGD-related infections. While the additional adult patient has sustained high levels of DHR+ neutrophils (77.2% at 6 months), the response of the newly treated pediatric patients has been similar to that of Patient 5 with initial high levels of neutrophil recovery followed by a decline. It is unclear at present why the engraftment of gene-marked cells was poor in these pediatric patients and whether the mechanisms were similar (due to pre-existing disease and concomitant drug therapies) or unrelated (immunological or technical).

Early attempts at gene therapy for CGD with γ-RV vectors achieved some transient therapeutic benefits, but in several cases were associated with clonal leukoproliferation[5,615]. Here, integration-site analysis in blood cells revealed highly polyclonal engraftment of gene-corrected stem cells, with no clonal expansion associated with enriched integration near cancer-associated genes[5,7] (Fig. 3a, 3b and Extended Data 4). In a previous γ-RV trial, methylation of CpG dinucleotides within the vector promoter sequence resulted in silencing of gene expression. The chimeric myeloid promoter in G1XCGD responds to transcription factors present mostly in mature myeloid cells and drives sufficient expression of gp91phox to reconstitute oxidase production in blood granulocytes and monocytes[8]. No silencing or methylation was detected. In each patient, all blood cell lineages had similar levels of gene marking, with the exception of T cells that had lower frequencies and lower diversity of vector integrants (Extended Data 3). This latter finding may reflect a lack of lymphodepletion in the conditioning regimen.

The level of reconstitution of phagocyte oxidase function required to mediate a meaningful clinical effect can be estimated from studies of female carriers of X-CGD, patients with X-CGD with small amounts of residual NADPH-oxidase activity (who have been shown to exhibit a significant survival advantage compared with patients with complete absence of oxidase activity), and from preclinical vector assessments[6,16–18]. On that basis, we predict that long-term functional correction of more than 10% of circulating myeloid cells with oxidase activity per cell approaching the normal range will provide lasting clinical benefit. The level of benefit may approach normal resistance to infection at or above 20% of circulating myeloid cells corrected, although individual factors may be influential. In this study, a target threshold of 10% was demonstrated in the six surviving adult patients, and above 20% in five of these six surviving adult patients. Quantitative assessment of superoxide production in engrafted neutrophils confirmed sustained activity. Clinical efficacy could in the future be improved with higher titer vector preparations or the use of transduction enhancers, and by avoiding the loss of primitive HSPC in the autologous graft, which may already be compromised by chronic inflammation[19,20].

The advantages of autologous HSC gene therapy over HSCT includes the avoidance of graft-versus-host disease and other alloreactive complications, and reduced complexity of

conditioning regimen. These results demonstrate promising effective autologous gene therapy in severely affected patients with X-CGD without evidence of genotoxicity. Further studies are warranted to formally assess longer term clinical efficacy and safety of G1XCGD in patients with X-CGD.

Methods

Study design and investigational therapy

Inclusion and exclusion criteria for the UK and US studies are detailed in Supplementary Table S1 In brief, male patients with X-linked chronic granulomatous disease (X-CGD), aged 2 years and older (>6 months for UK protocol), with molecular diagnosis of X-CGD confirmed by DNA sequencing and supported by laboratory evidence for absent or significantly reduced biochemical activity of the nicotinamide adenine dinucleotide phosphate (NADPH)-oxidase, and absence of 10/10 human leukocyte antigen (HLA)-matched donor (sibling or unrelated) were eligible.

The primary objective of the UK and US studies included evaluation of safety and the evaluation of efficacy and stability by biochemical and function reconstitution in progeny of engrafted cells at 12 months. The secondary objectives differed slightly between the two trials, and included clinical efficacy and evaluation of augmented immunity against bacterial and fungal infection (UK protocol), evaluation of immunologic reconstitution and patient health (US protocol) and assessment of hematopoietic stem cell transduction and engraftment (both protocols). Primary and secondary objectives are detailed more fully in Supplementary Table S1.

The protocol and informed consent documents were reviewed and approved or accepted by the US National Institutes of Health Recombinant DNA Advisory Committee, the UK Gene Therapy Advisory Committee, and the local institutional ethical and biosafety review boards at all participating clinical sites. The studies were performed in the USA under Food and Drug Administration-approved investigational new drug (IND) BB#16141; Medicines and Healthcare Products Regulatory Agency (MHRA) approved EudraCT Number 2012-000242-35 in the UK, and are registered at Clinicaltrials.gov ([USA] NCT02234934, [UK] NCT01855685). Genethon sponsored the UK trial and acquired exclusive rights for the commercial exploitation of the data generated under the US trial; during the trial, Orchard Therapeutics obtained an exclusive license from Genethon to certain rights and intellectual property related to the lentiviral vector G1XCGD, including clinical data, and named this program OTL-102.

The procedural schemas for the clinical trials are shown for the use of either fresh cells or cryopreserved cells (Fig. 1b, 1c). Cryopreserved cells were used increasingly over fresh cells as the studies progressed. The UK sites started using cryopreserved cells in 2016 and the US followed in 2018 in patients treated after those included in this manuscript. This was primarily for safety reasons as cryopreserved cells gave an extended shelf-life, which allowed full cell product characterization to be performed prior to initiation of conditioning. Following informed consent and eligibility confirmation, CD34+ cells recovered by bone marrow or apheresis were transduced ex vivo by the G1XCGD lentiviral vector. Patients

received busulfan myeloablative conditioning with pharmacokinetic monitoring. Drug products were infused intravenously through a central venous line over 30–45 minutes. Patient vital signs and clinical condition were monitored closely during and after the infusion for adverse reactions.

G1XCGD lentiviral vector production

Clinical lots of G1XCGD lentiviral vector[21] were produced at Genethon and Yposkesi (Evry, France). 293T cells were transfected with plasmids encoding the G1XCGD vector, HIV-1 gag/pol, HIV-1 rev, and the VSV-G glycoprotein. Culture supernatants were collected and processed using clarification, ion exchange chromatography, tangential flow filtration, gel filtration, formulation in X-Vivo 20 medium (Lonza), and aliquots were cryopreserved[22]. The titer of the vector preparations ranged between 2.1 and 3.3 E+09 IG (average 2.5 ± 0.5 E+09 IG/mL n = 5) genomes/mL, measured at Genethon using HCT116 colon carcinoma cells. Physical titers ranged between 1.3 and 3.8 E+04 ng P24/mL (average 2.4 ± 1.1 E+04 ng P24/mL n = 5) measured by enzyme-linked immunosorbent assay (ELISA). All lots of vector tested negative for replication competent lentivirus and met GMP release specifications.

G1XCGD lentiviral-vector-modified CD34+ cell product manufacturing—Cells were manufactured onsite at study sites in the US and UK (University of California, Los Angeles, USA; Boston Children's Hospital, USA; National Institutes of Health, USA; Great Ormond Street Hospital, UK). Harvested cells to use as back-up were collected from bone marrow isolation or mobilized peripheral blood. Mobilization of peripheral blood stem cells was accomplished by administration of granulocyte colony-stimulating factor (G-CSF) 10 μg/kg subcutaneously (SC) daily × 5 days, with leukapheresis performed on the fifth day. The back-up leukapheresis units were cryopreserved as per each site's standard operating procedure for standard hematopoietic progenitor cell products and stored in the vapor phase of liquid nitrogen (LN2) freezers. At least 1 month later, a second mobilization was performed to collect stem cells to manufacture the drug product. For some patients, cells for the back-up graft were obtained from the same mobilization used for manufacture of the drug product. On the fourth or fifth day of G CSF, a dose of plerixafor 0.24 mg/kg was administered intravenously 8–12 hours prior to leukapheresis, with a fifth dose of G-CSF given 2 hours prior to the apheresis. This collection was processed to isolate CD34+ cells using the CliniMACS system (Miltenyi Biotec, Germany). For some patients, a second leukapheresis was performed after a second dose of plerixafor on day 5 or 6, and a sixth dose of G-CSF was given on the sixth day of mobilization protocol.

Selected CD34+ cells were placed into cell culture in serum-free medium with recombinant human cytokines (stem cell factor, flt-3 ligand, thrombopoietin and interleukin-3). On the next 2 successive days, the G1XCGD vector was added to the cells in culture to a final concentration of 1E+08 IG/mL. The following day, the cells were removed from culture, washed twice, and formulated for intravenous administration. Samples were retained at multiple steps during the processing and from the final drug product (FDP). FDP was tested for sterility, gram-stain reactivity, endotoxin, mycoplasma, viability, CD34, and gp91phox surface expression by flow cytometry, colony-forming unit (CFU) numbers, and percentage

vector-insert+ CFU by polymerase chain reaction (PCR). Aliquots of the drug product were also grown in vitro for 7 days, followed by extraction of genomic DNA for vector copy number (VCN) determination by quantitative PCR (qPCR) or using digital droplet PCR (ddPCR) to measure the number of vector copies per human genome. In some patients, after regulatory approval of an amended manufacturing protocol, the drug product was cryopreserved in Cryostor 5 (5% dimethyl sulfoxide [DMSO], Sigma Aldrich) in Kryosure 20 bags (Saint-Gobain Performance Plastics), stored in vapor phase of LN2, and thawed at bedside immediately prior to administration.

Cell products and busulfan conditioning

Drug products were manufactured from G-CSF and Plerixafor-mobilized leukaphereses. A cryopreserved unmanipulated cell fraction was taken as back-up in the event of non-engraftment, and a CD34-selected cell preparation taken for G1XCGD transduction. In one case (Patient 8), freshly collected CD34+ cells were augmented with additional thawed autologous selected CD34+ cells that had been collected and frozen previously, to enable the initial required cell dose for transduction to be achieved. Collection of CD34+ cells was problematic in another patient (Patient 5), requiring three separate attempts (one aborted due to a systemic inflammatory reaction during administration of mobilizing agents). Drug product infused for the nine patients achieved final CD34+ cell doses of 6.5–32.6×106/kg (Table S2 Fig. S2). Transduction efficiency met release criteria for all cell products, with VCN ranging from 0.7 to 5.5 copies per cell (Table S2; Fig. S2b) in infused cells, indicating the secondary objective relating to evaluation of CD34+ hematopoietic cell transduction was met. For some products, the transduction efficiency of colony-forming units grown from the drug product were assessed for the presence of the vector by PCR; between 49.2 and 79.2% of the colonies were PCR-positive (Fig. S2c), indicating the primary objective to assess the efficacy in the progeny of engrafted cells was met. Busulfan was administered with pharmacokinetic drug monitoring and dosage adjustment leading to consistent dosing (Fig. S2d). Fresh cells post-transduction were administered within a few hours from the completion of processing, and cryopreserved cells were thawed at bedside and infused directly.

Pre-transplant cytoreductive conditioning—For cytoreductive conditioning, patients received intravenous busulfan twice daily for 3 days, starting at a dose of 2.0 mg/kg, and dose-adjusted based on pharmacokinetics to reach a total net area under the curve (AUC) for busulfan of 70,000–75,000 ng/mL*h. Serum busulfan levels were measured at intervals (immediately after infusion [time = 0] and at 0.5, 1, 2, 4 and 6 h) following the completion of the first infusion. Subsequent busulfan dosages were adjusted based on pharmacokinetic measurements to reach the target AUC on average over all doses, with busulfan levels re-measured after the final (6th) or penultimate (5th) busulfan dose to allow calculation of total busulfan exposure (Table 1; Fig. S2d).

Follow-up clinical and laboratory assessments

Upon recovery of neutrophils, follow-up evaluations were performed per the clinical protocol at 1, 2, 3, 6, 9, 12, 18 and 24 months after gene therapy (and continue to be monitored in long-term follow-up). Neutrophil NADPH-oxidase activity was measured by

standard methods16. CGD-related antibiotic therapy and antifungal therapies were discontinued when, in the opinion of the clinical team, adequate production of corrected neutrophils was evident and when pre-existing infections were deemed to have been cleared.

Promoter methylation analysis—Bisulfite conversion, PCR, sequencing, and bioinformatics analysis were performed at Eurofins Genomics Sequencing Europe (Konstanz, Germany). Bisulfite conversion was performed using the Zymo Research EZ 96 DNA Methylation Lightning Mag Prep kit (Zymo Research) according to manufacturer instructions. PCR was performed using a nested primer set to generate a 654bp fragment of the promoter region for sequencing. The PCR fragments were prepared for sequencing using the Eurofins Genomics Sequencing Europe standard protocols. Sequencing was performed on an Illumina HiSeq 4000 (Illumina, Inc.) to generate approximately 5 million 150bp read pairs for each sample. The sequencing reads were mapped to the promoter reference sequence using Bismark and Bowtie23,24. Methylation analysis was performed using the Bis-SNP adopted modules of GATK25–27.
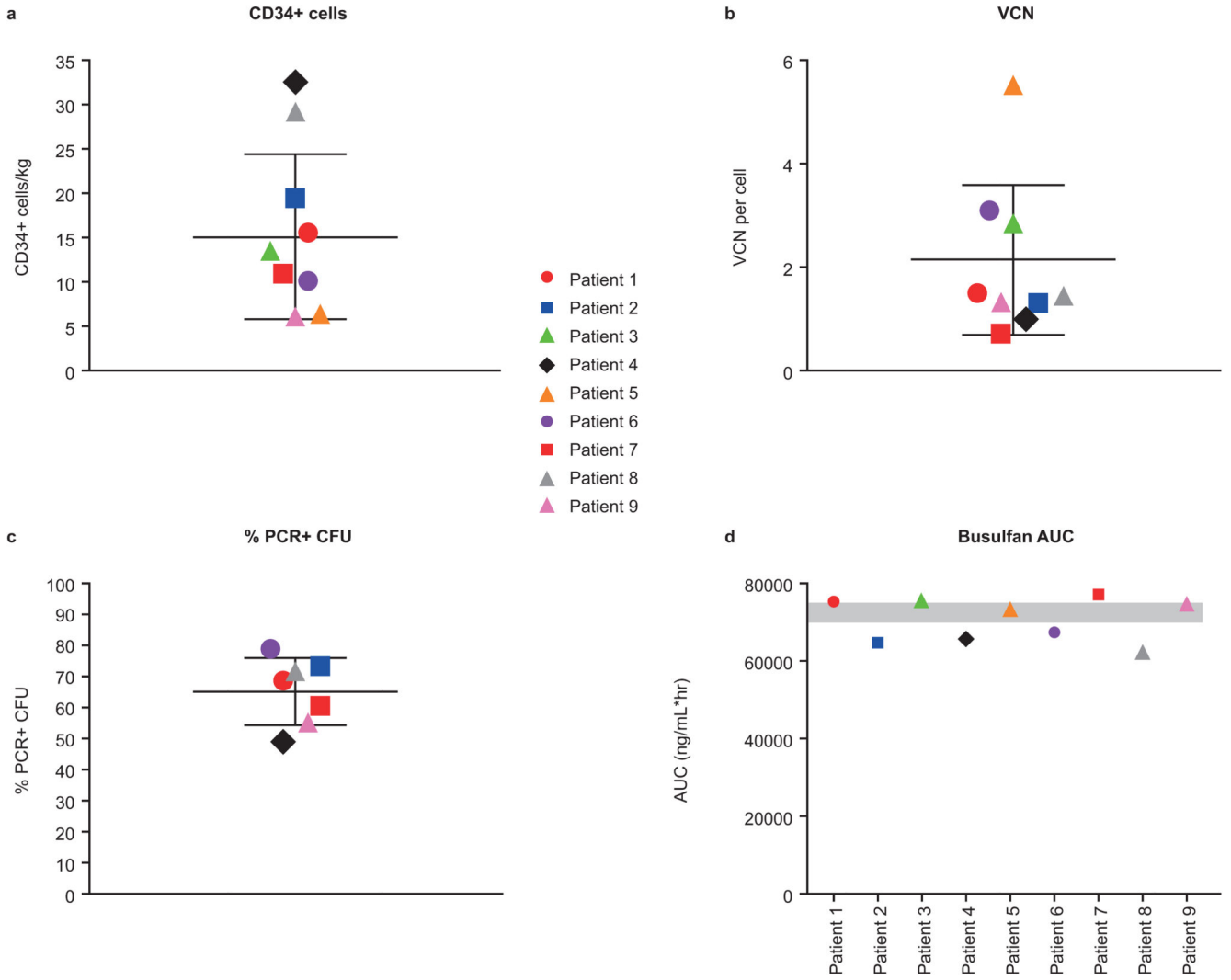
Analysis of integration target sites

For patients 2, 4, 6, 7 and 8, analysis of integration site distributions was carried out as described previously28,29. DNA was purified from transduction products prior to infusion or from blood cells from patients sampled longitudinally. DNA was cleaved by sonication, then DNA adaptors were ligated to the broken DNA ends. Two rounds of PCR were carried out to isolate host-vector DNA junction fragments. Each sample was analyzed four times independently to suppress PCR jackpotting. Samples were sequenced using the Illumina MiSeq. Analysis was carried out using the INSPIIRED pipeline29. Clonal structure was assessed using the sonic abundance method30, which uses information on the numbers of linker positions recovered per integration sites to count the numbers of cells sampled.

For patients 3, 5, and 9, integration sites were collected from Ficoll -purified granulocytes and fluorescence-sorted lymphocytes and monocytes through linear-amplification mediated (LAM)-PCR and high-throughput Illumina sequencing, as described previously31,32. Briefly, genomic DNA from isolated cell types was extracted (QIAamp DNA Blood Mini kit or Micro kit, QIAGEN), and whole -genome amplification was performed (Repli-G Mini Kit, QIAGEN) only on FACS-sorted lymphocytes as described previously33. A total of 300 ng of genomic DNA underwent two rounds of linear amplification (100 cycles in total) to enrich for vector long terminal repeat (LTR) -genome junctions, which were then captured using 5' biotinylated LTR specific primers and streptavidin magnetic beads. To follow, complementary strand synthesis was performed, then parallel digestion with three different restriction enzymes (MluCI, HpyCH4 IV and Aci I), and ligation to a linker cassette. The resulting fragments were then amplified by two additional exponential PCR steps. These LAM-PCR products were separated by gel electrophoresis on Spreadex high resolution gels (Elchrom Scientific) for visual inspection, and were pooled using barcoded adaptors in a library suitable for Illumina sequencing.

Available samples that passed our quality control of a minimum of 100 cells (by break-point analysis) were included in the analysis. The maximum relative clonal abundances in neutrophils was 2.3% and PBMC was 1.0% in the samples included.

Extended Data

Extended Data Fig. 1. Schematic representation of the transfer plasmid pCCL_chimGP91_WPRE_Kana

CMV promoter; R, R region of long terminal repeat (LTR); U5, Region unique to the 5' LTR; Psi, encapsidation sequence; RRE, rev responsive element; cPPT, central polypurine tract; CTSG, cathepsin G 5' minimal flanking regions; FES, human c-fes; coGP91, codon-optimized sequence CYBB gene which is translated into the cytochrome b-245, beta polypeptide; WPRE, mutated woodchuck hepatitis virus posttranscriptional regulatory element; PPT, HIV-1 polyadenylated region (post translational), dU3, region unique to the 3' LTR (U3) of the HIV-1 LTR, in which a 400 bp deletion (d) was introduced to inactivate the HIV-1 enhancer/promoter region; SV40 ori, Simian Virus 40 origin of replication; KANr, kanamycin resistance gene; COLE1, Colicin E1 resistance gene.

Extended Data Fig. 2. Cell products and busulfan conditioning
Panel a shows the final CD34+ cell products (left-axis) obtained for each patient. Panel b shows the VCN per infused cell post-transduction as determined by quantitative PCR. Transduction was also assessed by analyzing the percentage of vector CFUs PCR-positive for GX1CGD vector detected in the final cell product (Panel c). Vertical bars indicate mean and SD. Panel d displays the total net AUC busulfan exposure obtained by the sum of all pharmacokinetic measurements. Target total exposure of 70,000–75,000 ng/mL*h is indicated by the shaded area.

AUC, area under the curve; CFU, colony-forming unit; PCR, polymerase chain reaction; SD, standard deviation; VCN, vector copy number

a

Neutrophil DHR

n = 5 9 8 6   7   7   7   5   2

b

Neutrophil VCN

n = 8 6 8 8   7   7   7   6   4
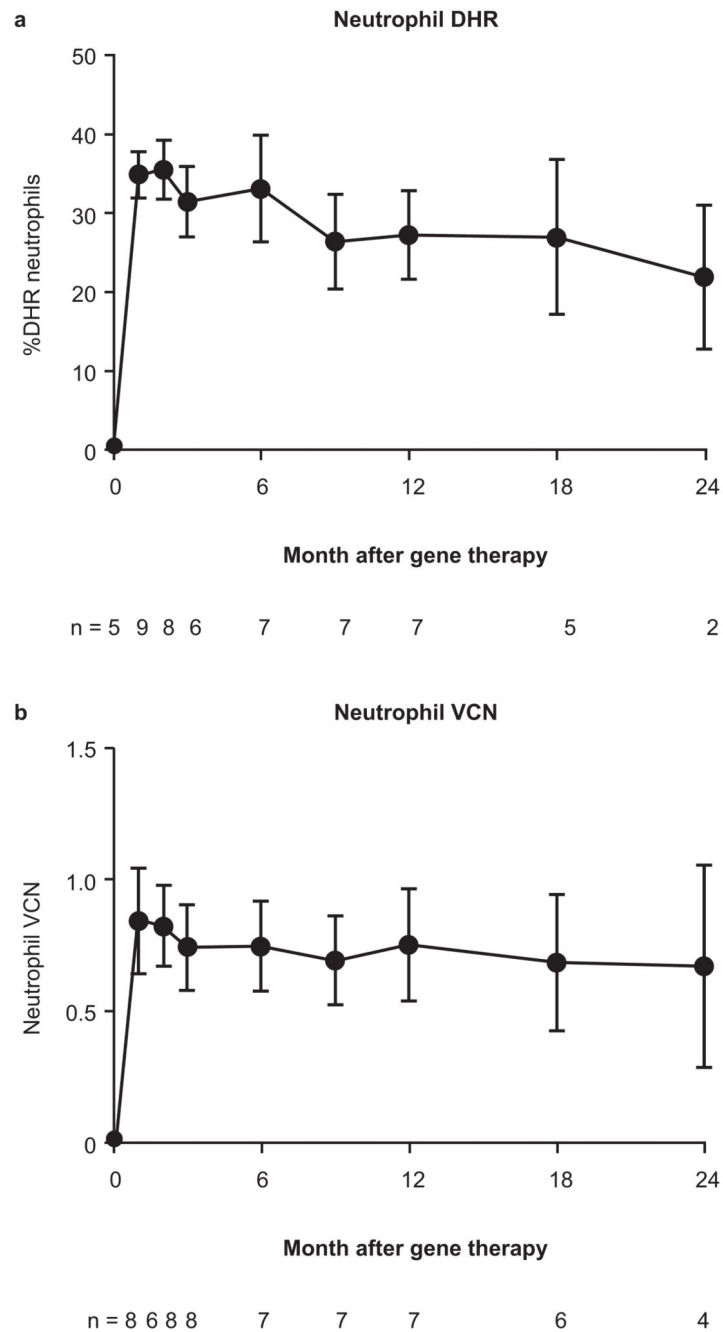
**Extended Data Fig. 3. Neutrophil DHR and VCN 24 months post treatment**
Panel a shows the mean (±SEM) of % DHR neutrophil up to 24 months post treatment, as measured by a dihydrorhodamine oxidation assay. Panel b shows the mean neutrophil VCN (±SEM) up to 24 months post treatment.

DHR, dihydrorhodamine; SEM, standard error of mean; VCN, vector copy number
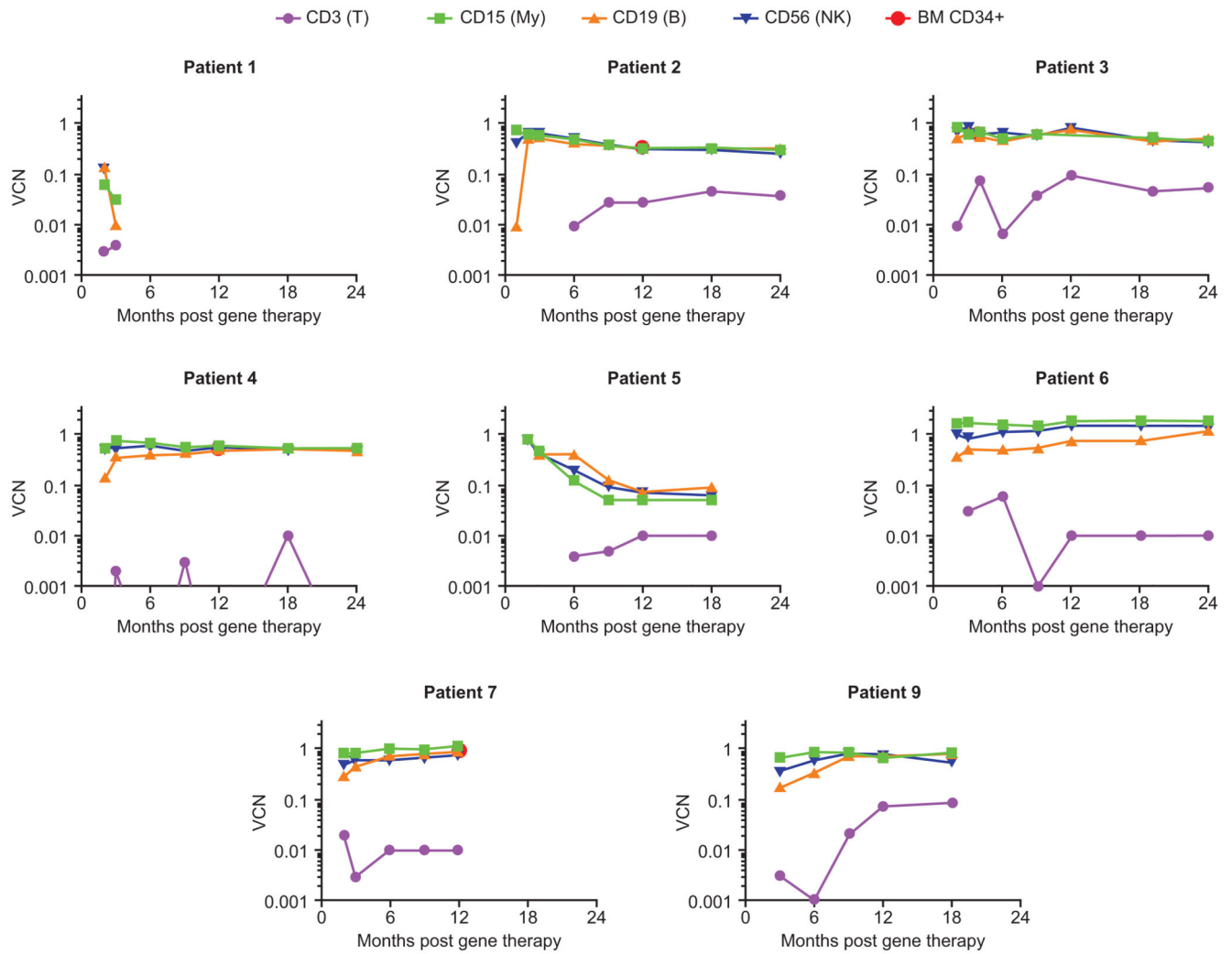
Extended Data Fig. 4. X-CGD lineage VCN
VCN determined by qPCR in multiple-cell lineages for patients surviving >1 month post-GT at each follow up, showing stable integration of vector into multiple immune cell types.
GT, gene therapy; qPCR, quantitative PCR; VCN, vector copy number
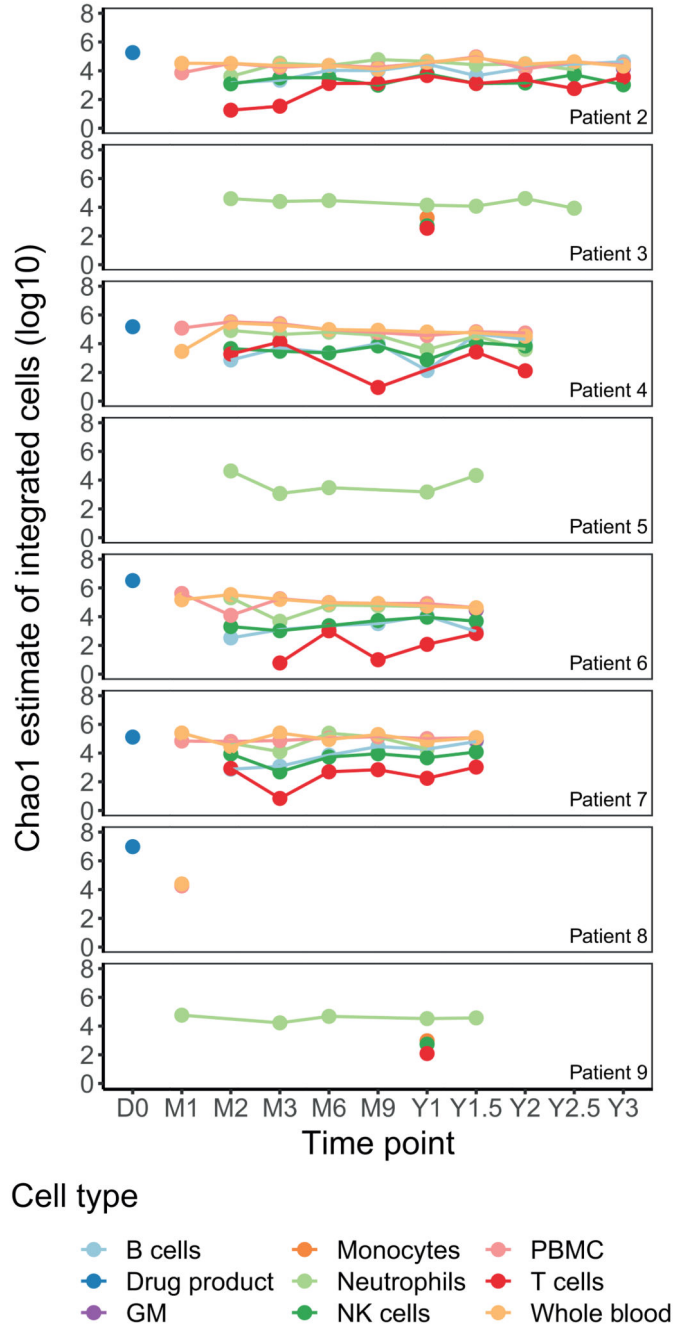
Extended Data Fig. 5. Longitudinal analysis of inferred minimal population sizes
Longitudinal analysis of minimal population size estimated using the CHAO1 method. The
x-axis shows time since cell infusion. D0 indicates the pre-infusion product. The y-axis
shows the numbers of unique integration sites (log scale). Cell types are color coded
(bottom). For a few patients a reduced number of cell types were available for analysis.
NK, natural killer; PBMC, peripheral blood mononuclear cell
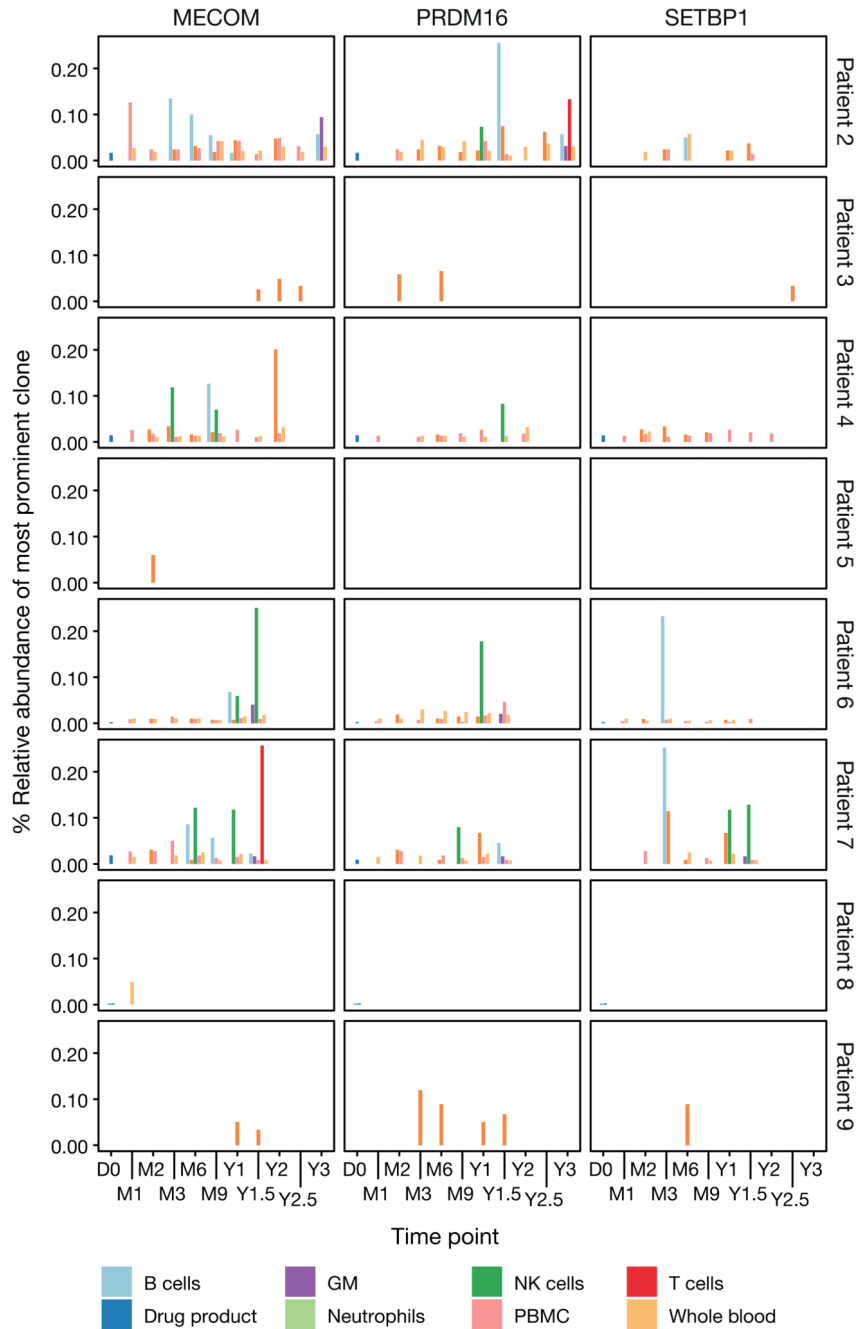
Extended Data Fig. 6. Catalogue of vector integration sites at genes of concern
Catalogue of cell clones with integration sites within MECOM (MDS/EVI1), PRDM16, and
SETBP2. These genes were chosen for analysis because they were targets of integration in
expanded cell clones in the first-RV-based CGD trial, and were implicated in adverse
outcomes. The x-axis shows the time point queried, the y-axis shows clonal abundance. Cell
types queried are color coded (key at the bottom). No cell clones with integration sites near
these genes of concern reaches   0.3% in abundance and there is no evidence for longitudinal
increases in proportion.

CGD, chronic granulomatous disease; γ-RV, gammaretroviral; NK, natural killer; PBMC, peripheral blood mononuclear cell

Supplementary Material

Refer to Web version on PubMed Central for supplementary material.

Acknowledgements

References

1. Winkelstein JA, et al. Chronic granulomatous disease. Report on a national registry of 368 patients. Medicine (Baltimore). 2000; 79:155–169. [PubMed: 10844935]

2. Holland SM. Chronic granulomatous disease. Hematol Oncol Clin North Am. 2013; 27:89–99. DOI: 10.1016/j.hoc.2012.11.002 [PubMed: 23351990]

3. Gungor T, et al. Reduced-intensity conditioning and HLA-matched haemopoietic stem-cell transplantation in patients with chronic granulomatous disease: a prospective multicentre study. Lancet. 2014; 383:436–448. DOI: 10.1016/S0140-6736(13)62069-3 [PubMed: 24161820]

4. Parta M, et al. Allogeneic reduced-iIntensity hematopoietic stem cell transplantation for chronic granulomatous disease: a single-center prospective trial. J Clin Immunol. 2017; 37:548–558. DOI: 10.1007/s10875-017-0422-6 [PubMed: 28752258]

5. Ott MG, et al. Correction of X-linked chronic granulomatous disease by gene therapy, augmented by insertional activation of MDS1-EVI1, PRDM16 or SETBP1. Nat Med. 2006; 12:401–409. DOI: 10.1038/nm1393 [PubMed: 16582916]

6. Kang EM, et al. Retrovirus gene therapy for X-linked chronic granulomatous disease can achieve stable long-term correction of oxidase activity in peripheral blood neutrophils. Blood. 2010; 115:783–791. DOI: 10.1182/blood-2009-05-222760 [PubMed: 19965657]

7. Stein S, et al. Genomic instability and myelodysplasia with monosomy 7 consequent to EVI1 activation after gene therapy for chronic granulomatous disease. Nat Med. 2010; 16:198–204. DOI: 10.1038/nm.2088 [PubMed: 20098431]

8. Santilli G, et al. Biochemical correction of X-CGD by a novel chimeric promoter regulating high levels of transgene expression in myeloid cells. Mol Ther. 2011; 19:122–132. DOI: 10.1038/mt.2010.226 [PubMed: 20978475]

9. Brendel C, et al. Non-Clinical efficacy and safety studies on G1XCGD, a lentiviral vector for *ex vivo* gene therapy of X-linked chronic granulomatous disease. Hum Gene Ther Clin Dev. 2018; 29:69–79. DOI: 10.1089/humc.2017.245 [PubMed: 29664709]

10. Schroder AR, et al. HIV-1 integration in the human genome favors active genes and local hotspots. Cell. 2002; 110:521–529. DOI: 10.1016/s0092-8674(02)00864-4 [PubMed: 12202041]

11. Berry CC, et al. Estimating abundances of retroviral insertion sites from DNA fragment length data. Bioinformatics. 2012; 28:755–762. DOI: 10.1093/bioinformatics/bts004 [PubMed: 22238265]

12. Dulamea AO, Lupescu IG. Neurological complications of hematopoietic cell transplantation in children and adults. Neural Regen Res. 2018; 13:945–954. DOI: 10.4103/1673-5374.233431 [PubMed: 29926815]

13. Simonis A, et al. Allogeneic hematopoietic cell transplantation in patients with GATA2 deficiency-a case report and comprehensive review of the literature. Ann Hematol. 2018; 97:1961–1973. DOI: 10.1007/s00277-018-3388-4 [PubMed: 29947977]

14. Weisser M, et al. Hyperinflammation in patients with chronic granulomatous disease leads to impairment of hematopoietic stem cell functions. J Allergy Clin Immunol. 2016; 138:219–228 e219. DOI: 10.1016/j.jaci.2015.11.028 [PubMed: 26853280]

15. Grez M, et al. Gene therapy of chronic granulomatous disease: the engraftment dilemma. Mol Ther. 2011; 19:28–35. DOI: 10.1038/mt.2010.232 [PubMed: 21045810]

16. Kuhns DB, et al. Residual NADPH oxidase and survival in chronic granulomatous disease. N Engl J Med. 2010; 363:2600–2610. DOI: 10.1056/NEJMoa1007097 [PubMed: 21190454]

17. Dinauer MC, Gifford MA, Pech N, Li LL, Emshwiller P. Variable correction of host defense following gene transfer and bone marrow transplantation in murine X-linked chronic granulomatous disease. Blood. 2001; 97:3738–3745. [PubMed: 11389011]

18. Marciano BE, et al. X-linked carriers of chronic granulomatous disease: Illness, lyonization, and stability. J Allergy Clin Immunol. 2018; 141:365–371. DOI: 10.1016/j.jaci.2017.04.035 [PubMed: 28528201]

19. Ribeil JA, et al. Gene therapy in a patient with sickle cell disease. N Engl J Med. 2017; 376:848–855. DOI: 10.1056/NEJMoa1609677 [PubMed: 28249145]

20. Thompson AA, et al. Gene therapy in patients with transfusion-dependent beta-thalassemia. N Engl J Med. 2018; 378:1479–1493. DOI: 10.1056/NEJMoa1705342 [PubMed: 29669226]

21. Zanta-Boussif MA, et al. Validation of a mutated PRE sequence allowing high and sustained transgene expression while abrogating WHV-X protein synthesis: application to the gene therapy of WAS. Gene Ther. 2009; 16:605–619. DOI: 10.1038/gt.2009.3 [PubMed: 19262615]

22. Merten OW, et al. Large-scale manufacture and characterization of a lentiviral vector produced for clinical ex vivo gene therapy application. Hum Gene Ther. 2011; 22:343–356. DOI: 10.1089/hum.2010.060 [PubMed: 21043787]

23. Krueger F, Andrews SR. Bismark: a flexible aligner and methylation caller for Bisulfite-Seq applications. Bioinformatics. 2011; 27:1571–1572. DOI: 10.1093/bioinformatics/btr167 [PubMed: 21493656]

24. Langmead B, Trapnell C, Pop M, Salzberg SL. Ultrafast and memory-efficient alignment of short DNA sequences to the human genome. Genome Biol. 2009; 10:R25.doi: 10.1186/gb-2009-10-3-r25 [PubMed: 19261174]

25. Liu Y, Siegmund KD, Laird PW, Berman BP. Bis-SNP: combined DNA methylation and SNP calling for Bisulfite-seq data. Genome Biol. 2012; 13:R61.doi: 10.1186/gb-2012-13-7-r61 [PubMed: 22784381]

26. McKenna A, et al. The Genome Analysis Toolkit: a MapReduce framework for analyzing next-generation DNA sequencing data. Genome Res. 2010; 20:1297–1303. DOI: 10.1101/gr.107524.110 [PubMed: 20644199]

27. DePristo MA, et al. A framework for variation discovery and genotyping using next-generation DNA sequencing data. Nat Genet. 2011; 43:491–498. DOI: 10.1038/ng.806 [PubMed: 21478889]

28. Sherman E, et al. INSPIIRED: A pipeline for quantitative analysis of sites of new DNA integration in cellular genomes. Mol Ther Methods Clin Dev. 2017; 4:39–49. DOI: 10.1016/j.omtm.2016.11.002 [PubMed: 28344990]

29. Berry CC, et al. INSPIIRED: Quantification and visualization tools for analyzing integration site distributions. Mol Ther Methods Clin Dev. 2017; 4:17–26. DOI: 10.1016/j.omtm.2016.11.003 [PubMed: 28344988]

30. Berry C, Hannenhalli S, Leipzig J, Bushman FD. Selection of target sites for mobile DNA integration in the human genome. PLoS Comput Biol. 2006; 2:e157.doi: 10.1371/journal.pcbi.0020157 [PubMed: 17166054]

31. Biasco L, et al. In Vivo tracking of human hematopoiesis reveals patterns of clonal dynamics during early and steady-state reconstitution phases. Cell Stem Cell. 2016; 19:107–119. DOI: 10.1016/j.stem.2016.04.016 [PubMed: 27237736]

32. Scala S, et al. Dynamics of genetically engineered hematopoietic stem and progenitor cells after autologous transplantation in humans. Nat Med. 2018; 24:1683–1690. DOI: 10.1038/s41591-018-0195-3 [PubMed: 30275570]

33. Biasco L, et al. In vivo tracking of T cells in humans unveils decade-long survival and activity of genetically modified T memory stem cells. Sci Transl Med. 2015; 7:273ra213.doi: 10.1126/scitranslmed.3010314

Editorial Summary

Initial results from phase I/II lentiviral gene therapy trials provide early evidence supporting its safety and efficacy in treating patients with X-linked chronic granulomatous disease.
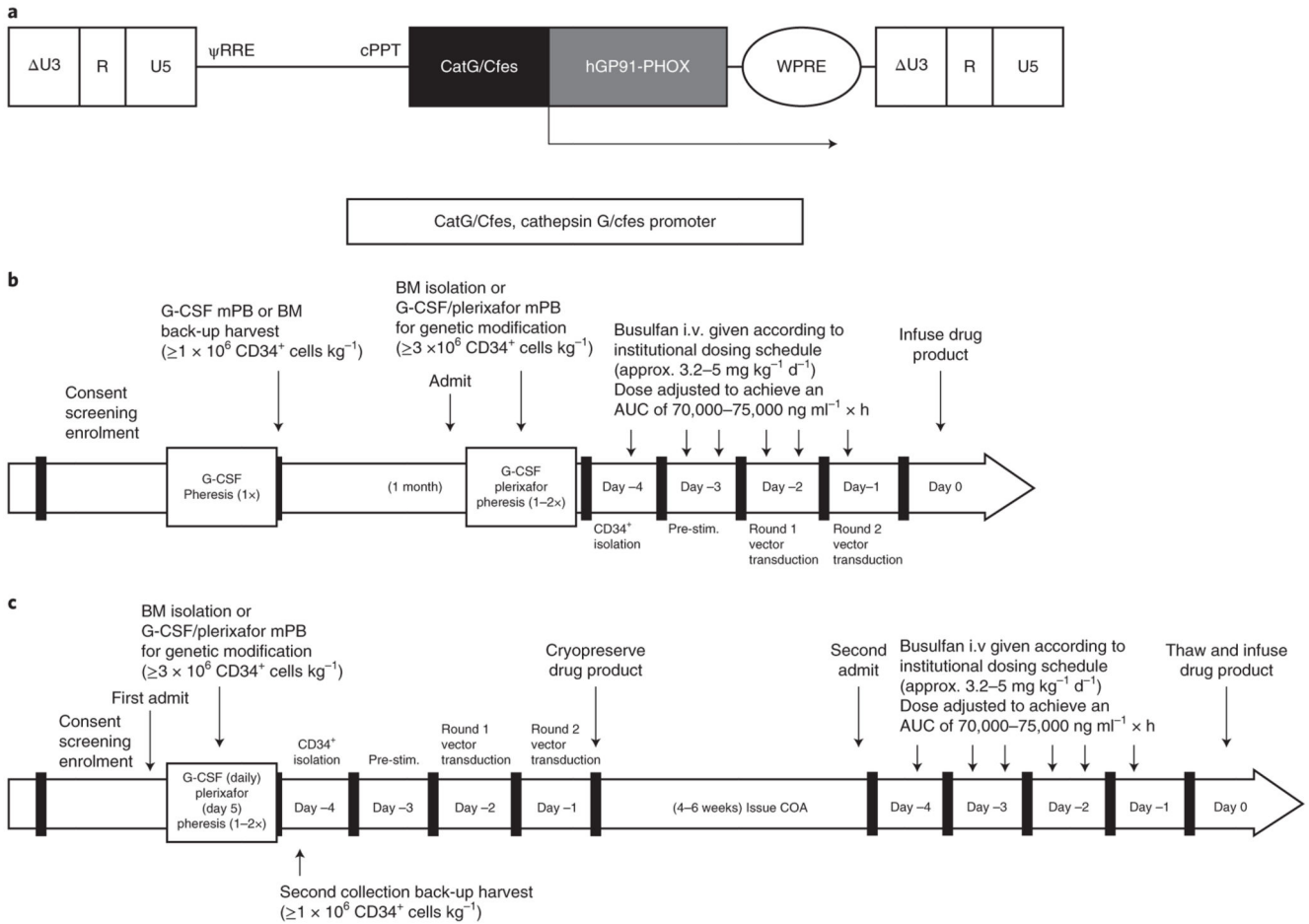
Fig. 1. Materials and methods (vector map and procedures)

Panel a displays the schematic representation of the G1XCGD lentiviral vector (LV) used to transduce CD34+ peripheral blood and bone marrow stem and progenitor cells in which expression of a codon-optimized human *CYBB* cDNA encoding for gp91phox is controlled by a chimeric regulatory element containing the Cathepsin G and Cfes gene promoter/enhancers, with a downstream WPRE to boost expression. **Panels b** and **c** show the schemas for the fresh cell and frozen/cryopreserved cell procedures, respectively. Differences between the two procedures include the timing of the primary harvest and back-up 'rescue' harvest of CD34$^+$ cells, the timing of G1XCGD vector addition, and that the cryopreservation procedure allowed full cell product characterization and release criteria to be met before cytoreductive conditioning was performed.

AUC, area under the curve; BM, bone marrow; CatG/Cfes, *CTSG* encoding Cathepsin G and the *FES* gene encoding Cfes; COA, certificate of analysis; G-CSF, granulocyte colony-stimulating factor; LV, lentiviral vector; mPB, mobilized peripheral blood; WPRE, Woodchuck hepatitis virus post-transcriptional regulatory element
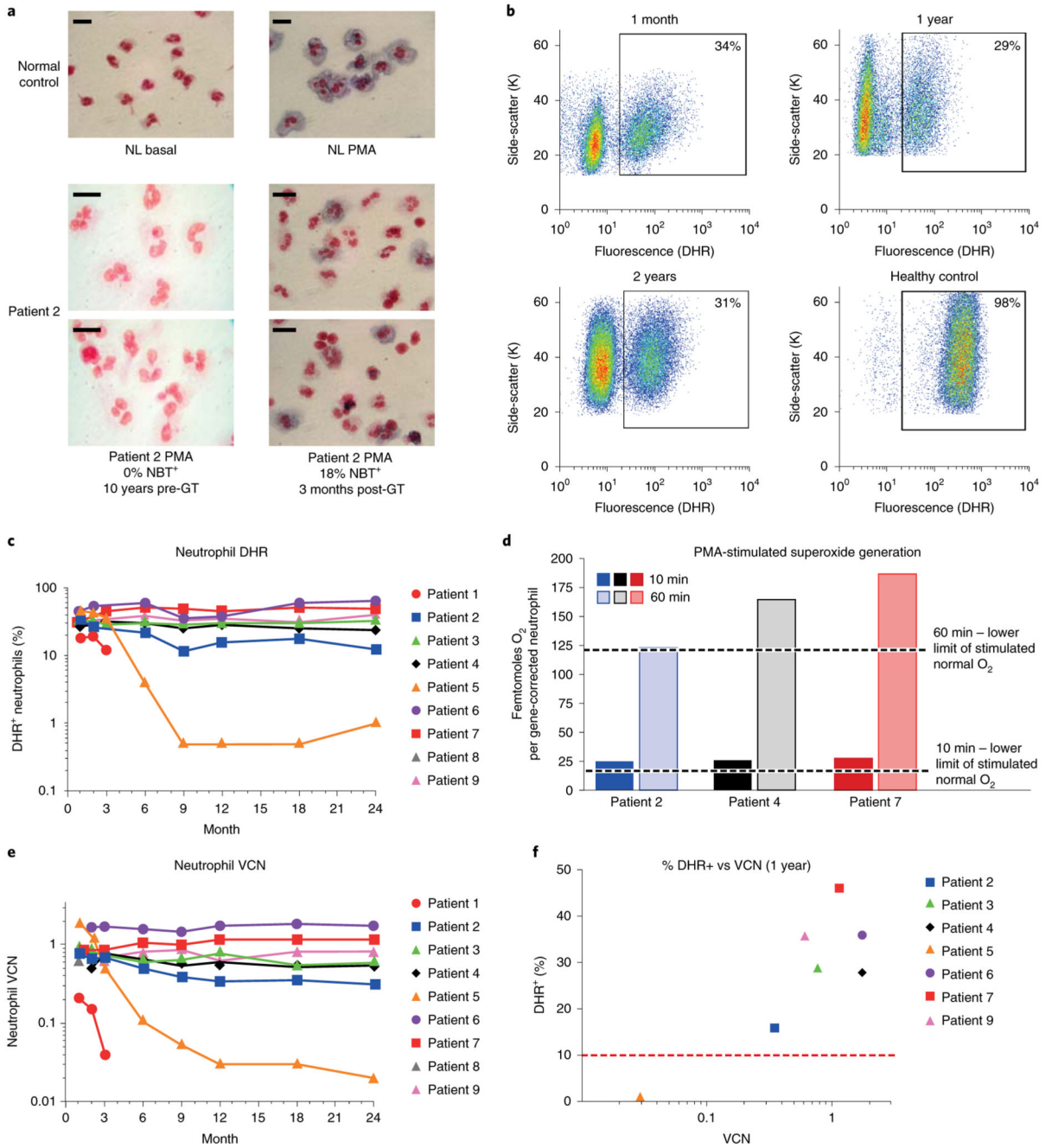
Fig. 2. Biochemical and clinical evidence of successful engraftment

Panel a shows the nitro-blue tetrazolium (NBT) test to detect functional circulating neutrophils from a peripheral blood sample from Patient 2 pre-gene therapy (left) and at 3 months after receiving gene therapy with G1XCGD (right). Generation of superoxide leads to reduction of NBT and formation of dark blue formazan precipitates in the observed cells. The scale bar measures approximately 10 micrometres; mature human neutrophils on a blood smear have an average diameter of 12–15 micrometres. **Panel b** shows the results of DHR fluorescence flow cytometry assaying functional oxidase activity in neutrophils over a

2-year period in Patient 3 post-gene therapy, and in a healthy control. After neutrophil stimulation with PMA (right), the fraction of DHR+ neutrophils were quantified. The percentage of DHR+ neutrophils in all treated patients at each time point is shown in **Panel c**. NAPDH-oxidase activity was quantified by measurement of neutrophil-stimulated reduction of ferricytochrome c, corrected for the percentage of oxidase-positive cells. Data for Patients 2, 4 and 7 are shown in **Panel d** following 10 minutes and 60 minutes of stimulation with PMA. The lower limit of normal superoxide generation for each timepoint is indicated by the dashed line. **Panel e** shows the neutrophil VCN for all patients measured at each time point for which data were available. VCN remained stable for six of seven surviving patients but decreased over time for one patient (Patient 5), who remains clinically well at follow-up with antimicrobial support. **Panel f** shows the percentage of DHR+ neutrophils versus granulocyte VCN for the seven surviving patients at 12 months. R^2=0.44; the dashed line represents 10% DHR.

NBT, nitroblue tetrazolium; DHR, dihydrorhodamine; GT, gene therapy; NL, normal; PMA, phorbol myristate acetate; VCN, vector copy number
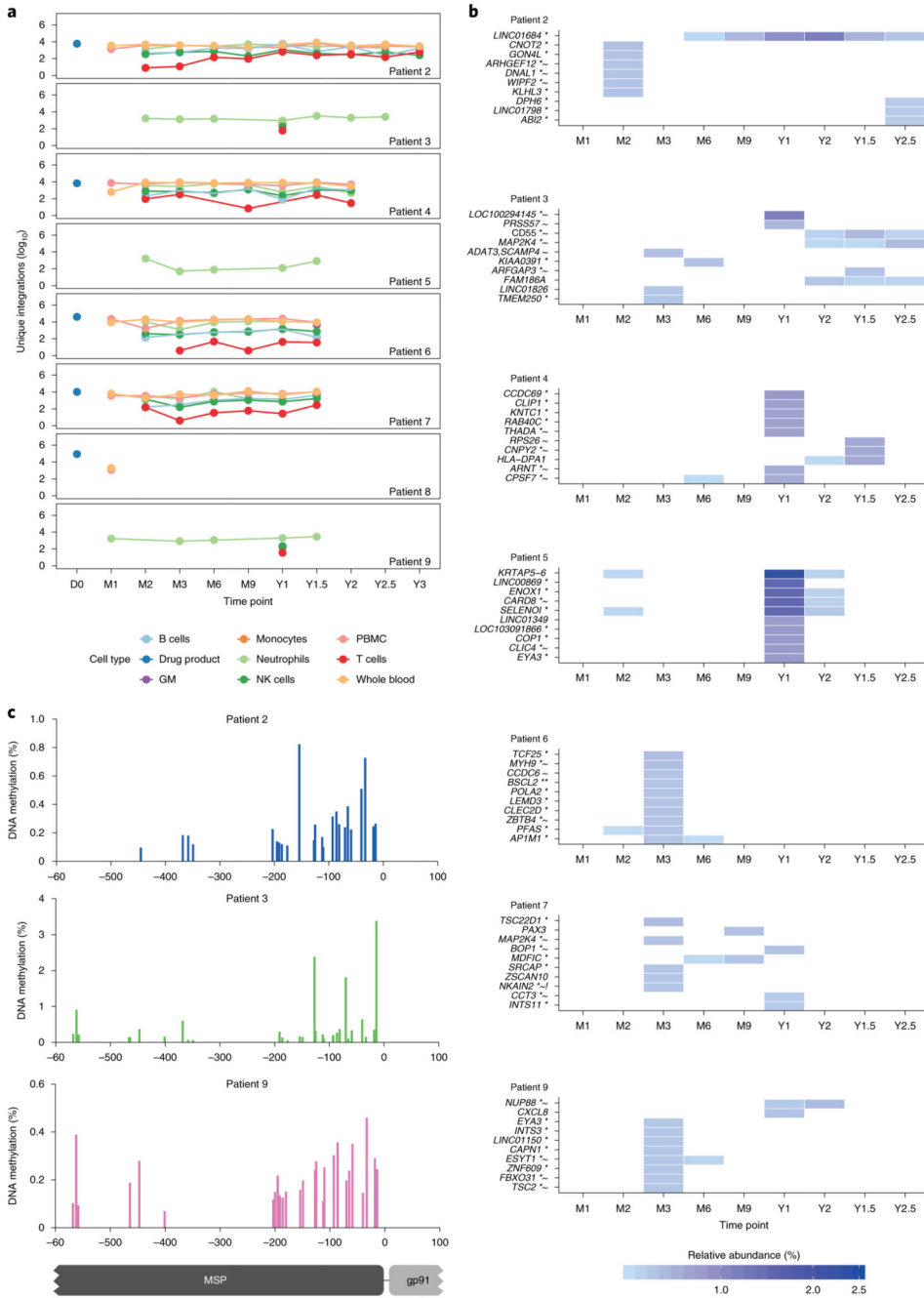
Fig. 3. Analysis of vector integration-site distributions and promotor methylation
Panel a shows longitudinal analysis of unique cell clones contributing to each cell type, inferred from counts of unique integration sites. The x-axis shows time since cell infusion. D0 indicates the pre-infusion product. The y-axis shows the numbers of unique integration sites (log scale). Cell types are color coded (bottom). For a few patients a reduced number of cell types were available for analysis. **Panel b** is a heat map illustrating the most abundant clones in each patient and their longitudinal behavior. Neutrophils were selected for this analysis because previous adverse events in CGD gene therapy with γ-RV vectors involved

outgrowth of myeloid cells. The x-axis shows the time post-treatment. The rows show cell clones, named by the nearest human gene (labels on left of figure). The relative abundance is shown by the heat map scale (bottom of figure). Quantification was carried out using fragment lengths to estimate abundance [11]. In **Panel c**, methylation of CpG dinucleotides is shown in Patients 2, 3 and 9 at 2.5 years, 18 months and 9 months post-gene therapy, respectively. The x-axis shows the positions of CpG dinucleotides relative to the gp91 mini-gene. The y-axis shows the percentage of methylation at each position. The methylation levels across the CpG islands are low for all samples, indicating that the gp91 mini-gene is not transcriptionally repressed.

CGD, chronic granulomatous disease; MSP, myeloid-specific promoter; NK, natural killer; PBMC, peripheral blood mononuclear cell; PCR, polymerase chain reaction; VISA, longitudinal vector integration-site analysis.

Table 1

Patient demographics, pre-transplant conditioning, and outcome results

Pt. #	Center	Age (y)	Race (ethnicity)	X-CGD (CYBB) mutation	Prior medical history	Date of gene therapy (MM/Y Y)	Status at gene therapy	Busulfan conditioning AUC (ng/mL*h)	DHR+ granulocytes, %		Status at last follow-up
									At 12 months	At last follow-up	
1	GOSH	4	Caucasian	c.1027A>C (p.Ther343Pr)	Pneumonectomy, EBV, *Aspergillus*, organomegaly, lymphadenopathy	7/13	Ongoing fever, organomegaly and lymphadenopathy	75873	–	12 (3 mo)	Death (at 3 mo) due to hyper-acute idiopathic pneumonitis
2	BCH	22	Caucasian	c.664 C>T (p.His222Tyr)	Klebsiella lymphadenitis MRSA liver abscess, lung abscess, Nocardia abscess, Serratia abscess, GI and urethral granulomas	12/15	No active infections at gene therapy	65117	16	13 (24 mo)	Clinically well, off antibiotic prophylaxis
3	GOSH	18	Mixed	c.1234_1257dup (p.Gly412_Ile419dup)	Osteomyelitis, cerebral hemorrhage, colitis, perianal fistula, perineal ulceration	7/16	Suspected fungal chest infection	75668	29	31 (24 mo)	Clinically well, off CGD-related antibiotic prophylaxis (remains on azithromycin)
4	NH	18	Caucasian (Hispanic)	c.1169 C>T (p.Pro390Leu)	Burkholderia cepacia Nocardia and *Aspergillus* pneumonias	7/16	Stable	66,191	28	25 (24 mo)	Clinically well, off antibiotic prophylaxis
5	GOSH	2	Asian (Korean)	c.469C>T (p.Arg157X)	Liver and splenic abscesses	4/17	Refractory spleen, liver abscesses, treatment with linezolid	73337	0.5	1 (24 mo)	Clinically well; receiving antimicrobial support (oral clindamycin and clarithromycin); weaned off steroids; gut improvement
6	UCLA	27	Asian	c.1314+2 T>A (Homozygous T>A at splice site exon 10 ([downstream 2 bases])	*Aspergillus*, Nocardia and Serratia pneumonia, IBD, Crohn's disease	4/17	Bronchiectasis and pulmonary fibrosis, lymphopenia	67666	36	63 (24 mo)	Infection-free, off CGD-related antibiotic prophylaxis (remains on TMP/SMX); has pneumothoraces requiring treatment (pre-existing condition); Crohn's and IBD improved (no active inflammation)

Pt. #	Center	Age (y)	Race (ethnicity)	X-CGD (CYBB) mutation	Prior medical history	Date of gene therapy (MM/YY)	Status at gene therapy	Busulfan conditioning AUC (ng/mL*h)	DHR+ granulocytes, %		Status at last follow-up
									At 12 months	At last follow-up	
7	NIH	24	Black/African American	c.676 C>T (p.Arg226x)	Multiple bacterial and fungal lung infections, lobectomy (lung), granulomatous liver, GI, recurrent lymphadenitis	6/17	Chronic persistent culture-positive Phellinus fungal pneumonia	77378	46	49 (24 mo)	Clinically well, off antibiotic prophylaxis
8	NIH	3	Caucasian (Hispanic)	c.374 G>A (p.Trp125Ter)	BCGosis . >1yr hx of disseminated Aspergillus (bone, lungs, CNS)	8/17	Resistant Aspergillus at gene therapy. Status post: multiple granulocyte transfusions	62349	–	44 (1 mo)	Death (at 1 mo) from cerebral bleed into pre-existing fungal infection site (pre-existing antiplatelet antibodies impeding post-conditioning platelet transfusions)
9	GOSH	22	Caucasian	c.271 C>T (p.Arg91X)	Cerebral Aspergilloma, colitis warts, granulomatous folliculitis; interstitia nephritis	9/17	Steroid-dependent colitis. Multifocal inflammatory changes on HRCT chest	75000	35	40 (24 mo)	Clinically well, off CGD-related antibiotic prophylaxis (remains on TMP/SMX); colitis resolved; being weaned off oral steroid; HRCT chest findings resolved; intermittent skin rashes persist

AUC, area under the curve; BCH, Boston Children's Hospital, USA; CGD, chronic granulomatous disease; CNS, central nervous system; DHR+, dihydrorhodamine-positive granulocytes; EBV, Epstein-Barr virus; GI, gastrointestinal; GOSH, Great Ormond Street Hospital, UK; HRCT, high-resolution computed tomography; hx, history; IBD, inflammatory bowel disease; MRSA, Methicillin-resistant *Staphylococcus aureus*; NIH, National Institutes of Health, USA; TMP/SMX, trimethoprim-sulfamethoxazole UCLA, University of California, Los Angeles, USA; X-CGD, X-linked chronic granulomatous disease;